Noisy MRI Reconstruction via MAP Estimation with an Implicit Deep-Denoiser Prior

Nikola Janjušević¹, Amirhossein Khalilian-Gourtani², Yao Wang³, Li Feng¹,

Abstract—Accelerating magnetic resonance imaging (MRI) remains challenging, particularly under realistic acquisition noise. While diffusion models have recently shown promise for reconstructing undersampled MRI data, many approaches lack an explicit link to the underlying MRI physics, and their parameters are sensitive to measurement noise, limiting their reliability in practice. We introduce Implicit-MAP (ImMAP), a diffusion-based reconstruction framework that integrates the acquisition noise model directly into a maximum a posteriori (MAP) formulation. Specifically, we build on the stochastic ascent method of Kadkhodaie et al. and generalize it to handle MRI encoding operators and realistic measurement noise. Across both simulated and real noisy datasets, ImMAP consistently outperforms state-of-the-art deep learning (LPDSNet) and diffusion-based (DDS) methods. By clarifying the practical behavior and limitations of diffusion models under realistic noise conditions, ImMAP establishes a more reliable and interpretable baseline for diffusion-based accelerated MRI reconstruction.

Index Terms—Denoising diffusion generative model, inverse problems, deep-learning

I. INTRODUCTION AND BACKGROUND

Magnetic resonance imaging (MRI) is a widely used, non-invasive technique for the clinical diagnosis of conditions affecting many organs. However, a primary limitation of MRI is its slow acquisition speed, which is constrained by fundamental physical principles. To accelerate scanning, parallel imaging methods use multiple receiver coils to acquire undersampled k-space data, thereby reducing scan time and performing a regularized reconstruction at inference [1]. This regularization is traditionally guided by hand-crafted priors, however, recently end-to-end trained deep neural networks have shown state-of-the-art performance [2].

Another growing body of related literature is zero-shot deep denoising diffusion generative models (DDGMs) [3]–[8]. These models have emerged as a powerful class of methods for solving image inverse problems. In natural image domains, these models have demonstrated an exceptional ability to produce realistic and high-fidelity reconstructions. Fundamentally, diffusion models are trained to learn the score function, i.e. the gradient of the log-probability of the data distribution, through a denoising process that gradually removes noise from corrupted samples. By reversing this diffusion process, the models can generate samples from the learned data distribution and effectively recover images from incomplete or degraded measurements [6]. In MRI, diffusion-based approaches have

New York University Grossman School of Medicine, {\bar{1}}Radiology Department, \bar{2}}Neurology Department, \bar{2}}, New York, NY 10016, USA.

³New York University Tandon School of Engineering, Electrical and Computer Engineering Department, Brooklyn, NY 11201, USA.

Please send all correspondence regarding to this manuscript to N. Janjušević (email:nikola.janjusevic@nyulangone.org).

shown promising results in achieving high acceleration rates under simulated noise conditions [4]. However, DDGMs are typically formulated using stochastic differential equations or Markov chains, both of which are decoupled from the underlying MRI physics and the applicability of DDGMs to real-world MRI data with measurement noise introduced by the scanner remains largely unexplored.

In a series of recent publications [2], [9]–[11], we have introduced a framework for the interpretable design of deep denoisers that generalize effectively across, and even beyond, their training noise levels. We have further extended this framework to the problem of MRI reconstruction, demonstrating its applicability in both supervised and self-supervised learning settings. In this work, we extend these ideas to diffusion-based models and propose an interpretable construction framework for diffusion models tailored to MRI reconstruction. Specifically, we build upon and expand the formulation of diffusion models introduced in Kadkhodaie et al. [12] to address inverse problems in the presence of observation noise. We show state-of-the-art performance of the proposed approach on both synthetically added noise and real MRI acquisitions with scanner noise.

A. MRI Reconstruction Problem

We model our observations as a subsampled multicoil Fourier domain signal $\boldsymbol{y} \in \mathbb{C}^{N_sC}$, with C coils, of a ground-truth image $\boldsymbol{x} \in \mathbb{C}^N$, with fourier-sampling locations denoted by index-set Ω and coil-sensitivity maps $\boldsymbol{s} \in \mathbb{C}^{NC}$,

$$\mathbf{y}_c = \mathbf{I}_{\Omega} \mathbf{F}(\mathbf{s}_c \circ \mathbf{x}) + \mathbf{\nu}_c, \quad \forall \ c = 1, \dots, C,$$
 (1)

where ${\pmb F}$ is the N-pixel 2D-DFT matrix, \circ denotes elementwise multiplication, and ${\pmb I}_\Omega \in \{0,1\}^{N_s \times N}$ is the row-removed identity matrix with kept rows indicated by Ω . For simplicity, we consider our observations to be noise-whitened such that ${\pmb \nu}_c \sim {\cal N}(0,\sigma^2{\pmb I})$ is per-channel i.i.d. Gaussian noise with noise-level σ identical in each channel. We denote this observation model through the encoding operator ${\pmb A}$ defined such that ${\pmb y} = {\pmb A}{\pmb x} + {\pmb \nu}$. We say the observation is accelerated by a factor of $R = N/N_s$.

B. Stochastic Ascent with a Denoiser's Implicit Prior

In this section, we present the stochastic gradient descent algorithm with a denoiser's implicit prior of Kadkhodaie et al. [12]. Let z=x+n where $x\sim p$ and $n\sim g_{\sigma}=\mathcal{N}(0,\sigma^2\boldsymbol{I})$. Then we may obtain the following relation (Tweedie's Formula [12]) directly from expressing the

noisy image distribution p_{σ} as the convolution of the image distribution and the Guassian,

$$p_{\sigma}(z) = \int_{\mathbb{R}^N} g_{\sigma}(z - x) p(x) dx$$
 (2)

$$\sigma^2 \nabla_{z} \log p_{\sigma}(z) = \mathbb{E}[x|z] - z. \tag{3}$$

Now let f be an MMSE Gaussian-noise denoiser, ex. we trained a learned denoiser $f = \arg\min_{f} \mathbb{E}[\|\boldsymbol{x} - f(\boldsymbol{z}; \sigma)\|_{2}^{2}]$ across a range of noise-levels σ . Then $f(z;\sigma) \approx \mathbb{E}[x|z]$ and we have approximate access to the gradient of the logprobability of the noisy image distribution,

$$\sigma^2 \nabla_z \log p_{\sigma}(z) = \mathbb{E}[x|z] - z \approx f(z;\sigma) - z.$$
 (4)

Tweedie's formula (4) tells us that the MMSE estimate of the ground-truth x given a noisy z is achieved by a single gradient ascent step on the log-probability of p_{σ} , $\mathbb{E}[\boldsymbol{x}|\boldsymbol{z}] = \boldsymbol{z} + \sigma^2 \nabla_{\boldsymbol{z}} \log p_{\sigma}(\boldsymbol{z})$ with step-size σ^2 . However, p_{σ} is only a Gaussian-blurred version of our true image distribution p. The key-insight of Kadkhodaie et al. [12] is that we may interpret the score function of the noisy distribution, $\sigma^2 \nabla_z \log p_{\sigma}(z)$, as an approximate ascent direction on the true image distribution. If we take a fractional step in this direction, our new estimate will be closer to the true image distribution, less noisy $(\sigma \downarrow)$, and we will have access to an even more accurate ascent direction w.r.t. the true image distribution. Upon this insight, Kadkhodaie et al. [12] propose the following algorithm, which may be interpreted as a coarseto-fine gradient ascent on the log-probability,

$$z_{t+1} = z_t + h_t(f(z_t) - z_t) + \epsilon_t,$$
 (5)

with starting point $z_0 \sim \mathcal{N}(0, I)$, step-size $h_t \in [0, 1]$ and stochastic noise term $\epsilon_t \sim \mathcal{N}(0, \gamma_t^2 I)$ introduced to help escape local maxima. In the same work, Kadkhodaie et al. [12] extended their algorithm to handle conditioning on measurement data, y = Ax, by performing maximization of the log-posterior using Baye's rule, i.e, $\arg \max_{x} \log p(x|y) = \arg \max_{x} \log p(x) + \log p(y|x)$. However, their method relied on y being noise-free and having an easily SVD decomposable observation operator A, limiting its direct application to large-scale MR imaging inverseproblems.

In light of these limitations, in Section II we propose an extension of Kadkhodaie's measurement-conditioned stochastic ascent algorithm which accounts for measurement noise and the large-scale nature of the MRI encoding operator.

II. PROPOSED METHOD

A. The Implicit MAP Algorithm

Let $y = Ax + \nu$ where $\nu \sim \mathcal{N}(0, \Sigma_{\nu})$. We seek the to reconstruct x from y via obtaining a MAP estimate,

$$\mathbf{x}^{\diamond} = \underset{\mathbf{x}}{\operatorname{arg max}} \ p(\mathbf{x}|\mathbf{y})$$

$$= \underset{\mathbf{x}}{\operatorname{arg max}} \ \log p(\mathbf{x}) + \log p(\mathbf{y}|\mathbf{x}).$$
(6)

$$= \underset{\boldsymbol{x}}{\operatorname{arg max}} \log p(\boldsymbol{x}) + \log p(\boldsymbol{y}|\boldsymbol{x}). \tag{7}$$

We tackle this problem with a coarse-to-fine stochastic gradient ascent on the log-prior and log-likelihood functions,

$$\boldsymbol{z}_{t+1} = \boldsymbol{z}_t + h_t \sigma_t^2 \left(\nabla_{\boldsymbol{z}_t} \log p_{\sigma_t}(\boldsymbol{z}_t) + \nabla_{\boldsymbol{z}_t} \log p(\boldsymbol{y}|\boldsymbol{z}_t) \right) + \boldsymbol{\epsilon}_t,$$
(8)

using the prior implicitly encoded by a trained denoiser f to access the prior score function via Tweedie's formula (4). We switch to the notation to variable z to indicate that our intermediate variables z_t belong to the noisy image distribution, $z_t \sim p_{\sigma_t}$. To access the likelihood score-function, $\nabla_{z_t} \log p(y|z_t)$, we model z_t as a noisy version of our desired ground-truth signal, $z_t \sim \mathcal{N}(x, \sigma_t^2 I)$. Following [6], [8], we approximate the distribution of a denoised z_t , i.e. $f(z_t)$, with a Gaussian distribution (i.e. a Laplace Approximation),

$$f(\boldsymbol{z}_t) \sim \mathcal{N}(\mathbb{E}[\boldsymbol{x}|\boldsymbol{z}_t], \boldsymbol{V}_t),$$

where the variance-matrix V_t is a modeling parameter which we set to $V_t = \frac{\sigma_t^2}{1+\sigma_t^2} I$ in practice, following [8]. We derive the likelihood function as

$$p(\boldsymbol{y}|\boldsymbol{z}_t) = \mathcal{N}(\boldsymbol{y}|\boldsymbol{A}\mathbb{E}[\boldsymbol{x}|\boldsymbol{z}_t], \boldsymbol{\Sigma}_t),$$

where $\mathbf{\Sigma}_t = \mathbf{\Sigma}_y + A V_t A^H$. Taking the gradient of the loglikelihood yields,

$$\nabla_{\boldsymbol{z}_{t}} \log p(\boldsymbol{y}|\boldsymbol{z}_{t}) = -\nabla_{\boldsymbol{z}_{t}} \frac{1}{2} \|\boldsymbol{\Sigma}_{t}^{-1/2} \left(\boldsymbol{A} \, \mathbb{E}[\boldsymbol{x}|\boldsymbol{z}_{t}] - \boldsymbol{y}\right)\|_{2}^{2}$$

$$= -\nabla_{\boldsymbol{z}_{t}} \, \mathbb{E}[\boldsymbol{x}|\boldsymbol{z}_{t}]^{H} \boldsymbol{A}^{H} \boldsymbol{\Sigma}_{t}^{-1} \left(\boldsymbol{A} \, \mathbb{E}[\boldsymbol{x}|\boldsymbol{z}_{t}] - \boldsymbol{y}\right). \tag{9}$$

With $\mathbb{E}[\boldsymbol{x}|\boldsymbol{z}_t] \approx f(\boldsymbol{z}_t)$, we implement $\nabla_{\boldsymbol{z}_t} \mathbb{E}[\boldsymbol{x}|\boldsymbol{z}_t]^H \boldsymbol{v} \approx \boldsymbol{J}_t^H \boldsymbol{v}$ with a vector-jacobian product (VJP) with respect to our trained denoiser f^1 . This allows us to solve the symmetric linear system in the likelihood term (9) via the conjugate gradient method [8]. Lastly, we employ a stochastic noise term (ϵ_t) with stochasticity term $\beta \in (0,1]$ for purposes of escaping local minima, achieving the stochastic MAP estimation algorithm with implicit denoiser prior (ImMAP), shown in Algorithm 1.

B. Comparison of ImMAP to Other Diffusion-based Methods

Denoising diffusion generative models (DDGMs) are formulated by modeling the gradual transition of a noise-free image distribution p_0 into a distribution of pure noise p_T , either through a Markov-chain process or more generally as a continuous time stochastic differential equation with forward (corruption) process,

$$d\mathbf{x}_t = h(\mathbf{x}_t, t)dt + l(t)d\mathbf{W}_t, \tag{10}$$

with $x_0 \sim p_0$ and W_t denoting a Wiener process. Solving (10) backwards in time is then interpreted as obtaining a sample from the noise-free image distribution p_0 , for appropriately chosen h and l [6]. These equations can be easily extended to sampling from a conditional distribution $p_0(\boldsymbol{x}|\boldsymbol{y})$ given measurements u [6].

This formulation of DDGMs introduces a plethora of modeling choices/assumptions having solely to do with the SDE/Markov process, unrelated to any imaging inverse problem. In contrast, the derivation of ImMAP makes no such

¹The VJP operator is accessible via standard automatic differentiation libraries, often via a pullback function.

Algorithm 1: ImMAP

```
Input: y \sim \mathcal{CN}(Ax, \Sigma_y), \Sigma_y, A, f, \beta = 0.05,
                                                                             \sigma_L = 0.01, \ h_0 = 0.01
                      Output: x^{\diamond} = \arg \max_{x} \log p(x) + \log p(y|x)
     1 Draw z_0 \sim \mathcal{CN}(0, \boldsymbol{I})
     2 t = 1, \sigma_t^2 = 1
    3 while \sigma_t > \sigma_L do
                               // Denoising step and VJP Operator
                            \hat{\boldsymbol{z}}_t, \boldsymbol{J}_t^H \leftarrow \text{pullback}(f(\cdot, \sigma_t), \boldsymbol{z}_t)
                          \sigma_t^2 \leftarrow \|\hat{oldsymbol{z}}_t - oldsymbol{z}_t\|_2^2/N
                            \sigma_t | \mathcal{L}_t | \mathcal
                             oldsymbol{u}_t \leftarrow - \mathbf{J}_t^H oldsymbol{A}^H oldsymbol{v}_t
                                // Stochastic Gradient Ascent
                          h_t \leftarrow h_0 \frac{t}{1 + h_0(t-1)}
\gamma_t^2 \leftarrow \sigma_t^2 ((1 - \beta h_t)^2 - (1 - h_t)^2)
\epsilon_t \sim \mathcal{CN}(0, \gamma_t^2 \mathbf{I})
12 \mid oldsymbol{z}_{t+1} \leftarrow oldsymbol{\hat{z}}_t + oldsymbol{\hat{h}}_t \left( \hat{oldsymbol{z}}_t - oldsymbol{z}_t + \sigma_t^2 oldsymbol{u}_t 
ight) + oldsymbol{\epsilon}_t
13 t \leftarrow t+1
14 return x^{\diamond} = z_t
```

modeling assumptions and instead relies only on Tweedie's formula (4) [6] and MRI physics.

Recently, Chung et al. proposed Decomposed Diffusion Sampling (DDS) [4], a DDGM designed specifically for large scale noisy inverse problems. DDS is formulated as a Krylov-subspace method, relying on a "few-step" conjugate gradient method to keep its intermediate estimates close to a Krylov subspace tangent to the noisy image manifold. However, the existence of such a tangent space is not necessarily valid in practice, and their choice of number of conjugate-gradient steps is shown to greatly influence their algorithm's performance. Additionally, they introduce another hyperparameter γ to control the trade-off between data-consistency and their score-based denoiser, which we find in practice needs tuning for different different MRI acceleration factors.

III. RESULTS

A. Dataset and Experimental Settings

The performance of all models was evaluated on an internal MRI brain dataset consisting of T2w multicoil k-space data, 72 fully-sampled datasets were used for training with 8 used as a held-out test set. This data was used in two experimental settings: 1) the simulated measurement setting, where the fully-sampled coil- combined reconstruction serves as ground truth and is subsequently passed through a parallel MR observation operator (allowing us to meaningfully compute quantitative image-quality metrics), and 2) a retrospectively subsampled k-space setting, where the fully-sampled multi-coil k-space is subsampled along a single cartesian readout direction. In the latter case, the noise in each coil makes these measurements deviate from any specific measurement operator, and hence they represent experiments with real Gaussian noise.

B. Training and Implementation

We trained a single noise-adaptive denoiser f (using the LPDSNet architecture [2] with A=I) on the fully-sampled reconstructions of the T2w brain data with synthetic additive Gaussian white noise (AWGN) in the range $\sigma \in [0,0.5]$. This denoiser was used for both the ImMAP and DDS based inferences for fair comparison. Additionally, we trained separate end-to-end reconstruction networks (LPDSNet [2]) on noiseless R=12 simulated kspace and noisy R=8 collected kspace. We obtain estimated coil noise-covariance matrices Σ_y via a wavelet-based multicoil image domain based method, following [1]. Hyperparameters of ImMAP were set as shown in Algorithm 1, taking roughly 128 iterations per inference. Hyperparameters of DDS [4] were set as M=5, $\eta=0.8$, iterations (NFE) = 99 and γ set by performing a grid-search around author-reported $\gamma=0.95$, per acceleration rate R.

C. Simulated Noisy Measurement (setting 1)

Fig. 1 shows example results of the proposed ImMAP against the end-to-end LPDSNet [2] and the diffusion generative model DDS [4]. In the high-acceleration noiseless setting (R=12, σ =0), the proposed ImMAP recovered finer structural details and reduced blurring compared to LPDSNet, and more accurately reconstructed small structures than DDS. These results align with the natural image literature, confirming that diffusion-based priors improve reconstruction quality under high undersampling.

Fig. 2 shows the evaluation of our method (ImMAP) against the baseline SENSE [13] and the diffusion-based DDS under noisy conditions (R=8, σ =0.05). SENSE amplified noise, while DDS produced oversmoothed images that lost fine details. In contrast, ImMAP preserved structural sharpness and detail, despite using the same denoiser prior as DDS. Quantitatively, ImMAP achieved an average (NRMSE, SSIM) of (0.1335 0.9603) and DDS an average of (0.1495 0.9489). Furthermore, ImMAP achieves this performance without the hyperparameter tuning and sensitivity of DDS.

D. Retrospective Subsampling with Real Noise (setting 2)

Lastly, we evaluated all methods on a test set with R=8 retrospective k-space subsampling and real measurement noise. As shown in Figures 3 and 4, SENSE reconstructions exhibit significant noise amplification. LPDSNet yields overly smooth results, consistent with the tendency of end-to-end networks to suppress fine details. While both diffusion-based methods preserve structure without noise amplification, DDS produces more smoothed reconstructions than ImMAP, especially at higher accelerations. Visual inspection confirms that ImMAP recovers more anatomical detail, avoiding both noise and oversmoothing.

IV. CONCLUSION

We introduced ImMAP, a diffusion-based MRI reconstruction method that integrates acquisition physics directly into a MAP estimation framework. Experiments on both synthetic and real noisy data demonstrate that ImMAP outperforms

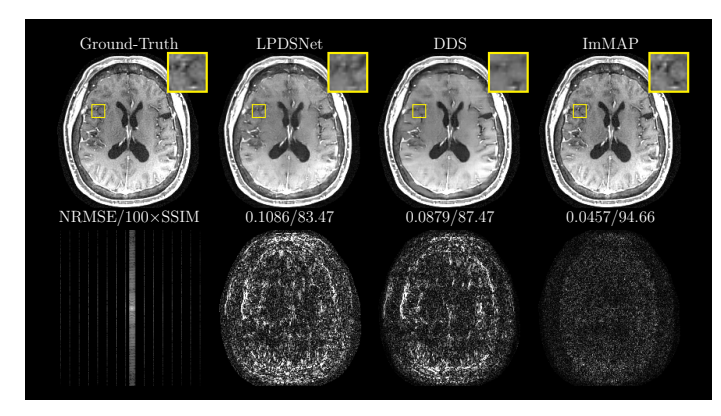


Fig. 1: Simulated $12\times$ accelerated reconstruction without added nosie ($\sigma=0$). (Top row, left to right) Ground-Truth: from which simulations are generated, LPDSNet, DDS, and proposed ImMAP reconstructions. (Bottom row, left to right): Input subsampled k-space (multicoil) and the reconstruction error for each method. Quantitative metrics (NRMSE/100xSSIM) are shown below each reconstruction.

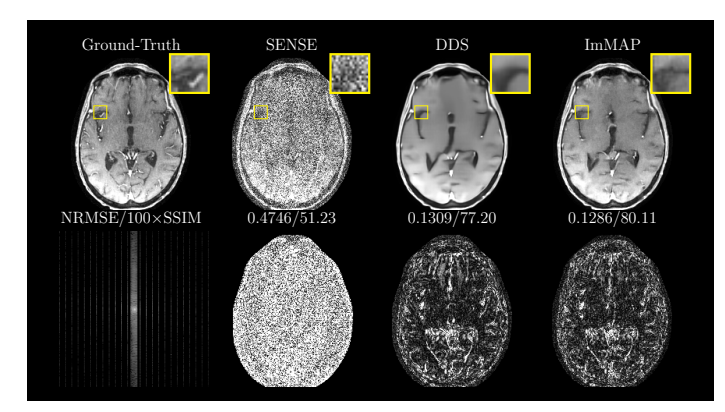


Fig. 2: Simulated $8\times$ accelerated reconstruction with added noise ($\sigma=0.05$). (Top row, left to right) Ground-Truth: from which simulations are generated, LPDSNet, DDS, and proposed ImMAP reconstructions. (Bottom row, left to right): Input subsampled k-space (multicoil) and the reconstruction error for each method. Quantitative metrics (NRMSE/100xSSIM) are shown below each reconstruction.

state-of-the-art deep learning and diffusion-based approaches, preserving anatomical detail without noise amplification or oversmoothing. Notably, it achieves robust performance without the parameter tuning/sensitivity of existing diffusion methods. Together, these results establish ImMAP as a reliable and interpretable baseline, clarifying the practical utility and limitations of diffusion models for accelerated MRI reconstruction.

ACKNOWLEDGMENTS

This work was supported in part by the NIH (R01EB030549, EB031083, R21EB032917, and P41EB017183) and was performed under the rubric of the Center for Advanced Imaging Innovation and Research (CAI2R), an NIBIB National Center for Biomedical Imaging and Bioengineering.

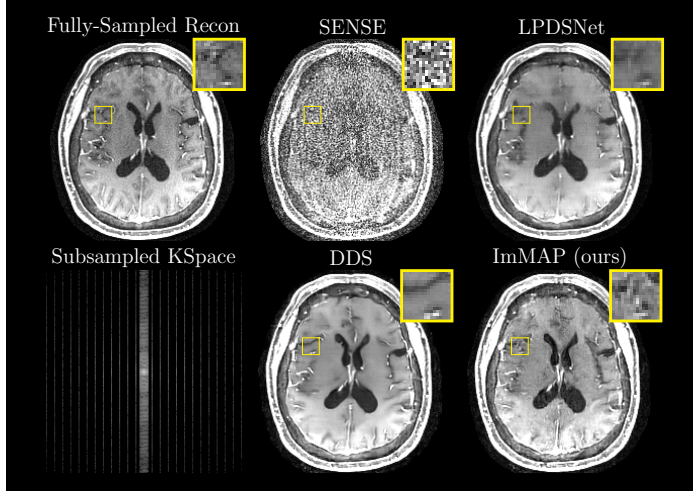


Fig. 3: Comparison of 8× accelerated reconstruction from retrospectively subsampled noisy k-space measurements. (Top row, left to right) Fully-sampled reconstruction. SENSE, LPDSNet reconstructions. (Bottom row, left to right): Input subsampled k-space (multicoil), DDS, and proposed ImMAP reconstructions. Quantitative metrics are not available as fully-sampled reconstruction does not correspond to ground-truth.

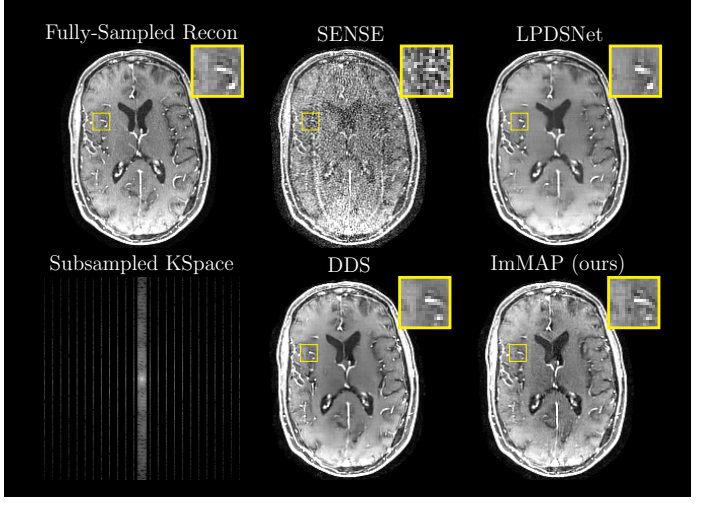


Fig. 4: Comparison of 8× accelerated reconstruction from retrospectively subsampled noisy k-space measurements. (Top row, left to right) Fully-sampled reconstruction. SENSE, LPDSNet reconstructions. (Bottom row, left to right): Input subsampled k- space (multicoil), DDS, and proposed ImMAP reconstructions. Quantitative metrics are not available as fully-sampled reconstruction does not correspond to ground-truth.

REFERENCES

- [1] N. Janjušević, J. Chen et al., "Self-supervised noise adaptive mri denoising via repetition to repetition (rep2rep) learning," Magnetic Resonance in Medicine, Nov. 2025. [Online]. Available: http://dx.doi.org/10.1002/mrm.70155
- [2] N. Janjušević, A. Khalilian-Gourtani et al., "Learned primal dual splitting for self-supervised noise-adaptive mri reconstruction," in 2025 IEEE 22nd International Symposium on Biomedical Imaging (ISBI), 2025, pp. 1–4.
- [3] Y. Zhu, K. Zhang et al., "Denoising diffusion models for plug-and-

SUBMITTED TO ISBI 2026 5

play image restoration," in *Proceedings of the IEEE/CVF conference on computer vision and pattern recognition*, 2023, pp. 1219–1229.

- [4] H. Chung, S. Lee, and J. C. Ye, "Decomposed diffusion sampler for accelerating large-scale inverse problems," in 12th International Conference on Learning Representations, ICLR 2024, 2024.
- [5] J. Ho, A. Jain, and P. Abbeel, "Denoising Diffusion Probabilistic Models," in *Advances in Neural Information Processing Systems*, vol. 33. Curran Associates, Inc., 2020, pp. 6840–6851.
- [6] G. Daras, H. Chung et al., "A survey on diffusion models for inverse problems," arXiv preprint arXiv:2410.00083, 2024.
- [7] F. Rozet, G. Andry et al., "Learning diffusion priors from observations by expectation maximization," in *The Thirty-eighth Annual Conference* on Neural Information Processing Systems, 2024.
- [8] J. Song, A. Vahdat et al., "Pseudoinverse-guided diffusion models for inverse problems," in *International Conference on Learning Represen*tations, 2023.
- [9] N. Janjušević, A. Khalilian-Gourtani, and Y. Wang, "CDLNet: Noise-Adaptive Convolutional Dictionary Learning Network for Blind Denoising and Demosaicing," *IEEE Open Journal of Signal Processing*, vol. 3, pp. 196–211, 2022.
- [10] ——, "Gabor is enough: Interpretable deep denoising with a gabor synthesis dictionary prior," in 2022 IEEE 14th Image, Video, and Multidimensional Signal Processing Workshop (IVMSP), 2022, pp. 1–5.
- [11] N. Janjusevic, A. Khalilian-Gourtani et al., "GroupCDL: Interpretable Denoising and Compressed Sensing MRI via Learned Group-Sparsity and Circulant Attention," 2024, arXiv:2407.18967.
- [12] Z. Kadkhodaie and E. Simoncelli, "Stochastic solutions for linear inverse problems using the prior implicit in a denoiser," *Advances in Neural Information Processing Systems*, vol. 34, pp. 13242–13254, 2021.
- [13] M. Uecker, P. Lai et al., "Espirit—an eigenvalue approach to autocalibrating parallel mri: Where sense meets grappa," Magnetic Resonance in Medicine, vol. 71, no. 3, p. 990–1001, May 2013.